

The Mechanism of O–O Bond Formation in Tanaka's Water Oxidation Catalyst**

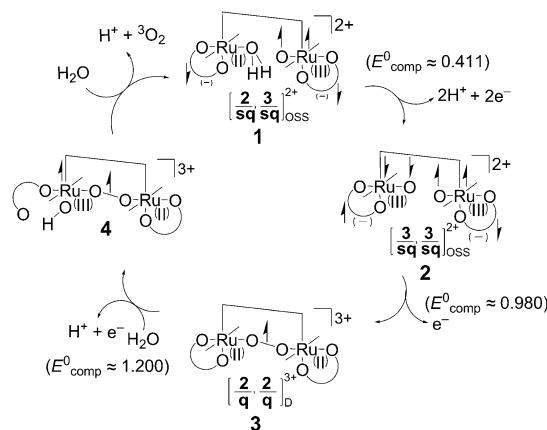
Soumya Ghosh and Mu-Hyun Baik*

The most appealing of the many strategies for meeting the ever-increasing demand for energy in a renewable fashion is to utilize solar energy.^[1] Artificial photosynthesis is a critical technology that may afford a permanent solution for both energy needs and to secure an inexhaustible supply of carbon-based chemical feedstocks.^[2] Solar energy is envisioned to drive the chemical reduction of carbon dioxide to ultimately give commodity chemicals that may be used as fuel. Inspired by natural photosynthesis, water oxidation is considered the ideal source for the electrons required to reduce one molecule of carbon dioxide. Recently, much progress was made on designing dinuclear,^[3] mononuclear,^[4] and tetranuclear^[5] homogeneous water oxidation catalysts. Our understanding of how to rationally design and systematically improve catalysts remains poor, however. The fundamental challenge is easy to identify: How can four electrons be removed efficiently from two oxo moieties to form molecular dioxygen and how do we promote O–O coupling under mild conditions?

The initial oxidation of water takes place commonly in a proton-coupled electron transfer process and is often accompanied by O–O bond formation to give a peroxo intermediate.^[6] In many catalytic systems this step is rate-determining, which is plausible, because bringing two oxygen atoms that are formally in the oxidation state –II in close proximity to each other is challenging. To enable rational strategies towards improving catalysts, we must better understand how currently known catalysts overcome this challenge in a conceptual sense. In previous work, we examined such a mechanism in Meyer's diruthenium-based blue dimer and found that the coupling of a metal-bound oxo with water, as first suggested by Hurst et al.,^[7] is most viable. We proposed that the $\{(bpy)_2Ru^{III}-OH_2\}$ fragment formally becomes a $\{(bpy)_2Ru^{IV}-O\}$ moiety in the catalytically competent intermediate, which engages in a radical recombination type of reaction with water to initially give an intermediate consisting of a $\{(bpy)_2Ru^{IV}-OOH\}$ fragment.^[8] This mechanism pro-

vided a plausible solution to the O–O coupling challenge and has since been recognized as one general reactivity pattern in water oxidation catalysis.

From a fundamental mechanistic perspective, Tanaka's complex, containing two quinone ligands attached to two ruthenium centers that are separated by a bis(terpyridine)-substituted anthracene linker, is intriguing. This spatially extended linker is not likely to promote direct electronic communication between the metal centers, whereas the presence of redox non-innocent quinone ligands^[9] is suggestive of a non-classical M–L electronic structure. Interestingly, Tanaka initially proposed that once the hydroxo group on each ruthenium center is deprotonated, the O–O bond may form in a non-rate-determining, spontaneous fashion.^[10] More recently, the O–O bond is hypothesized to form after the removal of two protons and two electrons.^[11] Previously, we identified the catalytically competent intermediate for Tanaka's complex in water to be **1**, which can be oxidized electrochemically in a single two-electron/two-proton coupled manner to afford intermediate **2** (Scheme 1).^[12] The redox active moiety is a $Ru^{II}-OH_2$ fragment, which becomes a $Ru^{III}-O$ moiety in the intermediate **2**.



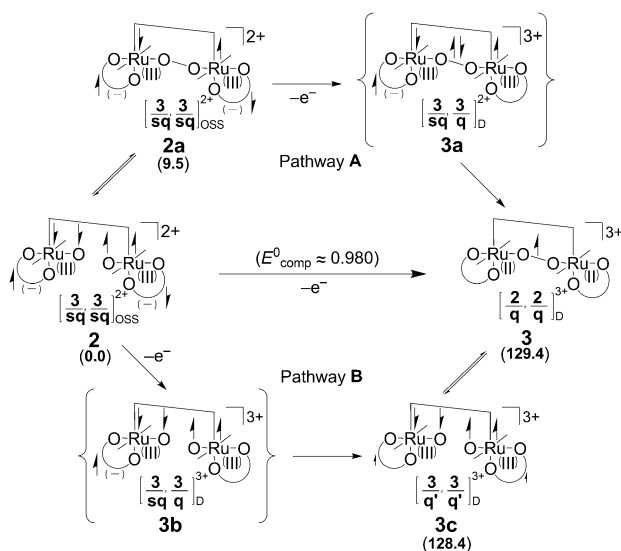
Scheme 1. Proposed catalytic cycle for the oxidation of water. sq = semiquinone, q = quinone, OSS = open-shell singlet, D = doublet.

The direct coupling of the two terminal oxyl radicals could form the μ^2 -peroxo intermediate **2a** (Scheme 2), traversing the transition state **2-TS** at 19.7 kcal mol⁻¹ (Supporting Information, Figure S2). But, this process is thermodynamically uphill by 9.5 kcal mol⁻¹ and we expect the peroxo intermediate to be a short-lived transient species. To push the dioxygen-evolving process forward, species **2a** must be oxidized electrochemically, and our calculations locate the

[*] S. Ghosh, Prof. Dr. M.-H. Baik
Department of Chemistry, Indiana University
800 E. Kirkwood Avenue, Bloomington, IN 47405 (USA)
and
Department of Chemistry, Korea University
208 Seochang, Chochiwon, Chung-nam 339-700 (South Korea)
E-mail: mbaik@indiana.edu
Homepage: <http://baik.chem.indiana.edu/>

[**] We thank the NSF (0116050 and CHE-0645381) for financial support. We also thank the Research Corporation for a Scialog Award (M.H.B.).

Supporting information for this article is available on the WWW under <http://dx.doi.org/10.1002/anie.201106337>.



Scheme 2. Two proposed pathways for the direct coupling of the two terminal oxyl radicals to form the μ^2 -peroxo species **3**.

oxidation product **3** at $119.9 \text{ kcal mol}^{-1}$, which corresponds to a computed redox potential of 0.568 V . Interestingly, the electronic structure of **3** reveals the presence of a μ^2 -superoxo moiety. As the μ^2 -(O_2)⁻ fragment is structurally protected by the ligand framework from contact with the electrode, it is difficult to envision how the direct oxidation of the transient peroxo moiety to its superoxo analogue is kinetically viable. We speculate that the initial electrochemical oxidation of **2a** occurs at the semiquinone ligand to give the hypothetical intermediate complex **3a** (Scheme 2), which contains one semiquinone ligand attached to a Ru^{III} center and a quinone group attached to the other Ru^{III} site, giving rise to an asymmetric charge distribution. The oxidative power of the newly formed $\{\text{Ru}^{\text{III}}(\text{q})\}$ fragment in **3a** is significantly enhanced compared to the $\{\text{Ru}^{\text{III}}(\text{sq})\}$ fragment in **2a**. This unbalanced electronic situation can be remedied by oxidizing the bridging peroxo ligand to a μ^2 -superoxo fragment in intermediate **3**, assisted by intramolecular electron transfer from the semiquinone group to its attached Ru^{III} center in **3a** (pathway A in Scheme 2). Whereas we could not locate species **3a** in our calculations, it is a plausible conceptual intermediate for the transformation of **2** \rightarrow **3** via **2a** and illustrates the role of the redox non-innocent quinone ligand as a mediator of the electron-transfer event during catalytic turnover.

A reasonable mechanistic alternative for the transformation of **2** \rightarrow **3** is to first remove an electron from species **2** without invoking the O–O bond formation, resulting in intermediate complex **3b** (pathway B in Scheme 2). The electronic imbalance described above is also present in this hypothetical intermediate. Our calculations identified an electronically relaxed complex **3c**, where the unpaired electron density of the semiquinone ligand has delocalized into the quinone ligand, reminiscent of a comproportionation event. As a result, both quinone/semiquinone ligands expose partial radical character that is halfway between that of a quinone and a semiquinone. Consequently, species **3c** exposes

an unusual electronic structure: the partial electron spin of the semiquinone/quinone ligand is antiparallel to one $\text{Ru}^{\text{III}}\text{--O}$ fragment and parallel to the other (Scheme 2). The most plausible pathway for reaching this thermodynamically viable intermediate directly from **2** involves intramolecular electron transfer from the semiquinone fragment in **3b** across the anthracene backbone to the quinone group, which is probably kinetically challenged. Thus, we conclude that pathway A is the most plausible scenario.

Structure **3c** is easily accessible via intermediate **3**, as the O–O bridge allows efficient communication between the two metal fragments and the energy difference between **3** and **3c** is only 1 kcal mol^{-1} . We located a transition state for the superoxo bond cleavage reaction **3** \rightarrow **3c** at $13.7 \text{ kcal mol}^{-1}$ (Supporting Information, Figure S3), suggesting that **3** and **3c** can coexist in an equilibrium state even at low temperatures. This behavior is analogous to the energetically more favorable peroxo bond cleavage reaction **2a** \rightarrow **2**, which is associated with a barrier of $10.2 \text{ kcal mol}^{-1}$, as discussed above. The trend that a peroxo bond, formally a single bond, is weaker than the superoxo bond, which will display some double-bond character, is intuitively understandable. The observation, however, that the O–O bond cleavage in **3** is such a facile process is surprising. Figure 1 compares the structural differences of **3** and **3c** and highlights the rigidity of

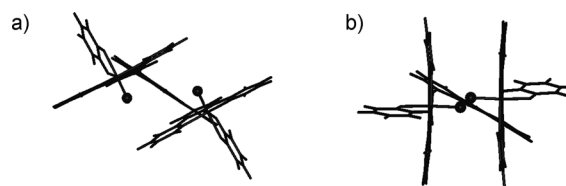


Figure 1. Structures of a) **3c** and b) **3** showing a view down the $\text{Ru}(\text{tpy})$ -anthracene vector. The oxygen atoms are shown as spheres.

the anthracene-bridged $[\{\text{Ru}(\text{tpy})(\text{q}/\text{sq})\}_2]$ framework: The O–O bond formation triggers a very similar twisting motion around the tpy-anthracene vector, which decreases the $\text{Ru}\cdots\text{Ru}$ distance. We propose that the function of the anthracene-bridged $[\{\text{Ru}(\text{tpy})(\text{q}/\text{sq})\}_2]$ framework is to maintain a close proximity of the two oxyl groups for the final dioxygen formation, despite the low thermodynamic driving force mentioned above for the peroxo and superoxo states. A structurally less-rigid system will likely open reaction channels that are energetically more favorable than the desired O–O bond coupling.

Next, the Ru–O bonds of the $\text{Ru}\text{--O}\text{--O}\text{--Ru}$ unit must be cleaved to release molecular dioxygen. The rigidity of the anthracene spacer and the strong $\text{Ru}^{\text{II}}\text{--O}$ bonds in **3** poses a problem for this process, however. The lowest transition state for the cleavage of the Ru–O bond in **3**, which we label as **3-TS**, was located at $34.2 \text{ kcal mol}^{-1}$ (Figure 2a). In the search for a more viable pathway for O_2 release, we considered further oxidizing one of the Ru centers to potentially generate a $\{\text{Ru}^{\text{III}}(\mu^2\text{-O}_2)\text{Ru}^{\text{II}}\}$ moiety, which we envisioned may remove an electron from the superoxo group to afford dioxygen. Surprisingly, removal of an electron from **3** gives

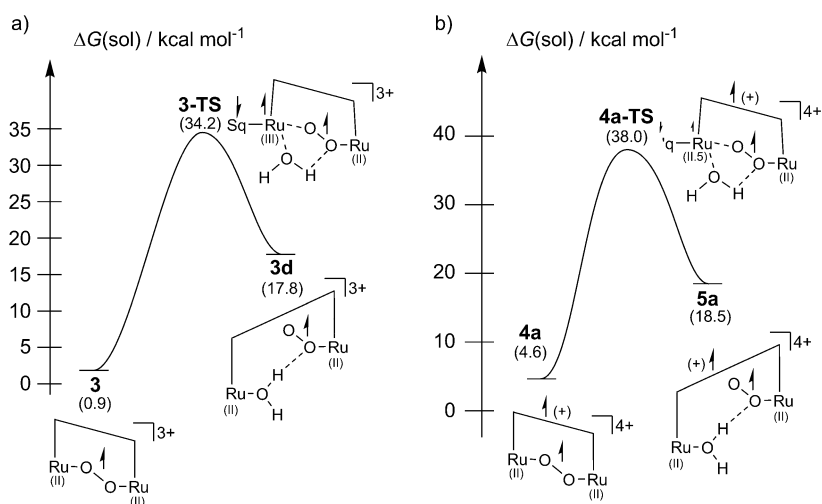
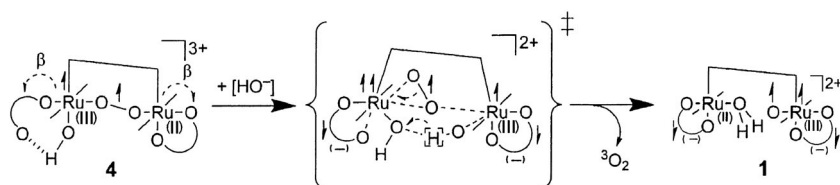


Figure 2. Reaction profiles for the cleavage of the ruthenium O–O bond by an incoming water molecule after the removal of a) three and b) four electrons.

intermediate **4a**, in which the $\{\text{Ru}^{\text{II}}(\mu^2\text{-O}_2^-)\text{Ru}^{\text{II}}\}$ framework is maintained and cationic radical character is generated on anthracene, indicating that the anthracene group is easier to oxidize than the $\{\text{Ru}^{\text{II}}(\mu^2\text{-O}_2^-)\text{Ru}^{\text{II}}\}$ fragment. The lowest energy barrier for cleaving the Ru–O(μ^2 -superoxo) bond in **4a** is associated with **4a-TS** at $38.0 \text{ kcal mol}^{-1}$ (Figure 2b). Thus, our calculations suggest that dioxygen release from intermediate **3** is improbable and simple oxidation of **3** does not afford a constructive intermediate, as it leads to the oxidation of anthracene that has little impact on the electronic structure of the reactive site of the catalyst.

After an extensive search of various plausible scenarios, we concluded that the most viable pathway of dioxygen release involves initial addition of a water molecule to one Ru^{II} center, which replaces a Ru–quinonoid bond to give intermediate **3e** (Figure 3) traversing the transition state at $25.6 \text{ kcal mol}^{-1}$ (Supporting Information, Figure S3). Subsequent removal of an electron and a proton affords intermediate **4**, traversing the transient intermediate species **4b**. As described above, the anthracene linker is still redox-active and **4b** also displays radical character on the anthra-



Scheme 3. Proposed pathway for the release of dioxygen.

release of dioxygen. We propose that this step involves a rearrangement of the η^1 -quinone moiety in **4** to a η^2 -quinone ligand along with the rotation of the hydroxo ligand. We envision that the $\text{Ru}^{\text{II}}\text{--O}(\text{superoxo})$ bond of the other subunit is replenished by a stronger $\text{Ru}^{\text{III}}\text{--OH}$ bond at the transition state. The quinone ligands play an important role again by accommodating an electron (Scheme 3) and lowering the barrier of the last step. Despite significant efforts, we were unable to locate a transition state for this process. Addition of a hydroxide ligand, which we may envision as addition of water concomitant to proton loss, to intermediate **4** readily leads to expulsion of dioxygen and recovery of complex **1**. This last process is either barrierless or associated with a low-energy transition state.

In summary, we propose that the oxidation of water to dioxygen, the Tanaka catalyst follows a reaction pathway that requires a characteristic reorganization of the coordination mode of the redox non-innocent quinone ligand. The ease of formation of the bridged superoxo complex **3** via

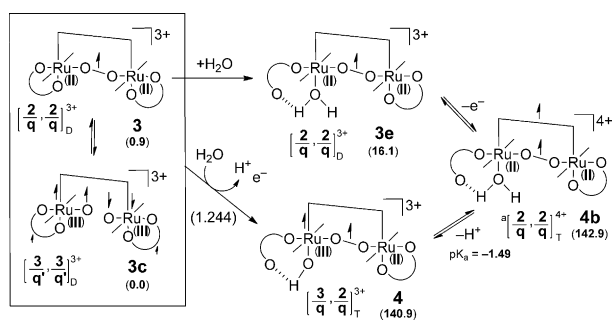


Figure 3. Proposal for the mechanism of the last redox event leading to dioxygen release.

an intramolecular radical coupling of the two terminal oxyl moieties in preference over an intermolecular reaction between the catalyst and a water molecule is rare.^[6b,14] There are several previous studies where O–O bond formation by the direct coupling of two Ru–O moieties has been proposed and confirmed by computational/experimental work.^[15] In these cases, the bridging peroxo moiety directly promoted communication between the two Ru^{III}/Ru^{IV} centers. Thus, reduction of the peroxo moiety to regenerate the catalyst and liberate dioxygen required no extra manipulation of the ligand environment. In other words, release of dioxygen was achieved without any active participation of the auxiliary ligands, in contrast to the mechanism proposed in the present study. Most mechanisms of catalytic water oxidation, on the other hand, invoke O–O bond formation events between a water molecule and a catalyst-bound oxyl moiety, which typically constitutes the most difficult step of the reaction. Tanaka's catalyst is distinctively different, because: 1) the terminal oxo moieties are buried inside a rigid catalyst framework and are not accessible to the solvent; 2) unlike the {Ru^{IV}–O}₂ moiety of Meyer's blue dimer, the {Ru^{III}–O}₂ core operative in Tanaka's catalyst lacks the driving force for directly cleaving the O–H bond of water in a homolytic fashion and has to resort to the mechanism we proposed above; and 3) the intramolecular O–O bond formation involves a smaller entropic penalty than the intermolecular mechanism involving a solvent water molecule and the metal-bound oxo moieties, but the release of dioxygen becomes more difficult, because the peroxo/superoxo intermediate is as a consequence relatively low in energy. To enable dioxygen release and escape the thermodynamic trap, Tanaka's complex must utilize the redox non-innocent nature of the quinone ligands.

Received: September 7, 2011

Revised: November 14, 2011

Published online: December 23, 2011

Keywords: density functional theory · redox non-innocence · ruthenium · water oxidation

- [1] a) N. S. Lewis, D. G. Nocera, *Proc. Natl. Acad. Sci. USA* **2006**, *103*, 15729–15735; b) N. S. Lewis, D. G. Nocera, *Proc. Natl. Acad. Sci. USA* **2007**, *104*, 20142–20142.
- [2] a) J. H. Alstrum-Acevedo, M. K. Brennaman, T. J. Meyer, *Inorg. Chem.* **2005**, *44*, 6802–6827; b) D. Gust, T. A. Moore, A. L. Moore, *Acc. Chem. Res.* **2009**, *42*, 1890–1898.
- [3] a) J. A. Gilbert, D. S. Eggleston, W. R. Murphy, D. A. Geselowitz, S. W. Gersten, D. J. Hodgson, T. J. Meyer, *J. Am. Chem. Soc.* **1985**, *107*, 3855–3864; b) Y. Naruta, M. Sasayama, T. Sasaki, *Angew. Chem.* **1994**, *106*, 1964–1965; *Angew. Chem. Int. Ed. Engl.* **1994**, *33*, 1839–1841; c) M. Ledney, P. K. Dutta, *J. Am. Chem. Soc.* **1995**, *117*, 7687–7695; d) J. Limburg, J. S. Vrettos, L. M. Liable-Sands, A. L. Rheingold, R. H. Crabtree, G. W. Brudvig, *Science* **1999**, *283*, 1524–1527; e) T. Wada, K. Tsuge, K. Tanaka, *Angew. Chem.* **2000**, *112*, 1539–1542; *Angew. Chem. Int. Ed.* **2000**, *39*, 1479–1482; f) C. Sens, I. Romero, M. Rodriguez, A. Llobet, T. Parella, J. Benet-Buchholz, *J. Am. Chem. Soc.* **2004**, *126*, 7798–7799; g) R. Zong, R. P. Thummel, *J. Am. Chem. Soc.* **2005**, *127*, 12802–12803; h) T. A. Betley, Q. Wu, T. V. Voorhis, D. G. Nocera, *Inorg. Chem.* **2008**, *47*, 1849–1861; i) Y. Xu, T. Åkermark, V. Gyollai, D. Zou, L. Eriksson, L. Duan, R. Zhang, B. Åkermark, L. Sun, *Inorg. Chem.* **2009**, *48*, 2717–2719.
- [4] a) J. J. Concepcion, J. W. Jurss, J. L. Templeton, T. J. Meyer, *J. Am. Chem. Soc.* **2008**, *130*, 16462–16463; b) N. D. McDaniel, F. J. Coughlin, L. L. Tinker, S. Bernhard, *J. Am. Chem. Soc.* **2008**, *130*, 210–217; c) H.-W. Tseng, R. Zong, J. T. Muckerman, R. Thummel, *Inorg. Chem.* **2008**, *47*, 11763–11773; d) J. D. Blakemore, N. D. Schley, D. Balcells, J. F. Hull, G. W. Olack, C. D. Incarvito, O. Eisenstein, G. W. Brudvig, R. H. Crabtree, *J. Am. Chem. Soc.* **2010**, *132*, 16017–16029; e) W. C. Ellis, N. D. McDaniel, S. Bernhard, T. J. Collins, *J. Am. Chem. Soc.* **2010**, *132*, 10990–10991; f) R. Lalrempuia, N. D. McDaniel, H. Müller-Bunz, S. Bernhard, M. Albrecht, *Angew. Chem.* **2010**, *122*, 9959–9962; *Angew. Chem. Int. Ed.* **2010**, *49*, 9765–9768; g) Z. Chen, J. J. Concepcion, T. J. Meyer, *Dalton Trans.* **2011**, *40*, 3789–3792; h) D. K. Dogutan, R. McGuire, D. G. Nocera, *J. Am. Chem. Soc.* **2011**, *133*, 9178–9180; i) D. J. Wasylenko, C. Ganesamoorthy, J. Borau-Garcia, C. P. Berlinguette, *Chem. Commun.* **2011**, *47*, 4249–4251.
- [5] a) Y. V. Geletii, B. Botar, P. Kögerler, D. A. Hillesheim, D. G. Musaev, C. L. Hill, *Angew. Chem.* **2008**, *120*, 3960–3963; *Angew. Chem. Int. Ed.* **2008**, *47*, 3896–3899; b) A. Sartorel, M. Carraro, S. Gianfranco, R. D. Zorzi, S. Geremia, N. D. McDaniel, S. Bernhard, M. Bonchio, *J. Am. Chem. Soc.* **2008**, *130*, 5006–5007; c) R. Brimblecombe, A. Koo, G. C. Dismukes, G. F. Swiegers, L. Spiccia, *J. Am. Chem. Soc.* **2010**, *132*, 2892–2894; d) L. Franca's, X. Sala, E. Escudero-Adán, J. Benet-Buchholz, L. s. Escriche, A. Llobet, *Inorg. Chem.* **2011**, *50*, 2771–2781; e) Z. Huang, Z. Luo, Y. V. Geletii, J. W. Vickers, Q. Yin, D. Wu, Y. Hou, Y. Ding, J. Song, D. G. Musaev, C. L. Hill, T. Lian, *J. Am. Chem. Soc.* **2011**, *133*, 2068–2071.
- [6] a) R. A. Binstead, C. W. Chronister, J. Ni, C. M. Hartshorn, T. J. Meyer, *J. Am. Chem. Soc.* **2000**, *122*, 8464–8473; b) S. Romain, L. Vigara, A. Llobet, *Acc. Chem. Res.* **2009**, *42*, 1944–1953.
- [7] J. K. Hurst, J. Zhou, Y. Lei, *Inorg. Chem.* **1992**, *31*, 1010–1017.
- [8] X. Yang, M.-H. Baik, *J. Am. Chem. Soc.* **2006**, *128*, 7476–7485.
- [9] a) K. Kobayashi, H. Ohtsu, T. Wada, T. Kato, K. Tanaka, *J. Am. Chem. Soc.* **2003**, *125*, 6729–6739; b) C. Remenyi, M. Kaupp, *J. Am. Chem. Soc.* **2005**, *127*, 11399–11413; c) J. T. Muckerman, D. E. Polyansky, T. Wada, K. Tanaka, E. Fujita, *Inorg. Chem.* **2008**, *47*, 1787–1802.
- [10] T. Wada, K. Tsuge, K. Tanaka, *Inorg. Chem.* **2001**, *40*, 329–337.
- [11] J. L. Boyer, J. Rochford, M.-K. Tsai, J. T. Muckerman, E. Fujita, *Coord. Chem. Rev.* **2010**, *254*, 309–330.
- [12] S. Ghosh, M.-H. Baik, *Inorg. Chem.* **2011**, *50*, 5946–5957.
- [13] The significant deviation of approximately 300 mV between the computed and experimental potentials for the fourth redox event can be attributed to the irreversible nature of this oxidation process, which makes an accurate measurement of the redox potential with standard electrochemical techniques impossible.
- [14] L.-P. Wang, Q. Wu, T. Van Voorhis, *Inorg. Chem.* **2010**, *49*, 4543–4553.
- [15] a) F. Bozoglian, S. Romain, M. Z. Ertem, T. K. Todorova, C. Sens, J. Mola, M. Rodríguez, I. Romero, J. Benet-Buchholz, X. Fontrodona, C. J. Cramer, L. Gagliardi, A. Llobet, *J. Am. Chem. Soc.* **2009**, *131*, 15176–15187; b) J. Nyhlén, L. Duan, B. Åkermark, L. Sun, T. Privalov, *Angew. Chem.* **2010**, *122*, 1817–1821; *Angew. Chem. Int. Ed.* **2010**, *49*, 1773–1777.